MID-INFRARED LASER ULTRASONIC TESTING FOR COMPOSITE MATERIALS

Masahiro KUSANO[1*], Hideki HATANO[1], Kanae OGUCHI[2],
Hisashi YAMAWAKI[1], Makoto WATANABE[1,2] and Manabu ENOKI[2]

[1]1-2-1, Sengen, Tsukuba, Ibaraki, Japan, National Institute for Materials Science
[2] 7-3-1, Hongo, Bunkyo, Tokyo, The University of Tokyo
[*] KUSANO.Masahiro@nims.go.jp

Keywords: Mid-infrared laser, Laser ultrasonic testing, Fiber reinforced plastics, Reflection mode, C-scan

ABSTRACT

Ultrasonic testing is the most common method to detect defects in materials and evaluate their sizes and depth. Since piezo-electric transducers are manually handled from point to point, it takes much time and labor costs for enormous products such as airplanes. Laser ultrasonic testing (LUT) is breakthrough technique. A pulsed laser generates ultrasonic waves on a material surface due to thermoelastic effect or ablation. In addition, ultrasonic waves can be detected by a laser interferometer. Thus, LUT can realize instantaneous inspection without contacting any probes with materials so that it has many advantages in high efficiency and extensive application.

A pulse laser with around 3.2 μm wavelength (mid-IR) is more suitable to generate ultrasonic waves for fiber reinforced plastics (FRPs) than other wavelength lasers because the light is prone to be well absorbed by the polymeric matrix. On the other hand, such a laser is not available in the market. Thus, we developed an efficient wavelength conversion device for emitting the mid-IR light by pumping an optical parametric oscillator using a compact Nd:YAG solid-state laser. Our LUT system composed of the Nd:YAG laser, the wavelength conversion device and the laser interferometer is most suitable for inspection of FRPs. The signal-to-noise ratio of ultrasonic waves generated by the mid-IR laser is higher than that by the Nd:YAG laser.

The purpose of the present study is to evaluate the performance of the mid-IR LUT system in reflection mode. We investigated the effects of the CFRP and the laser properties on the generated ultrasonic waves. In addition, C-scan images by the system were also presented.

1 INTRODUCTION

Carbon fiber reinforced plastics (CFRPs) have been extensively used as structural materials for airplanes and automobiles because of their high specific strength and corrosion resistance. As for airplanes, these last few years, the application expands to not only secondary structural components (e.g., flaps, tailplanes, engine covers) but also primary structural components such as a body and main wings. As CFRP products must pass higher level standard, non-destructive testing (NDT) for CFRP products both at manufacturing and in service are indispensable.

Ultrasonic testing (UT) is the most common method to detect defects in materials and evaluate their dimensions with wave analyses. Piezo-electric transducers are usually used to transmit and receive ultrasonic waves. Since a transducer needs to be tightly contacted with samples by a medium (e.g., gel, oil, and water) and to be manually handled from point to point, it takes much time and labor costs for huge products. Other methods for ultrasonic propagation and detection (e.g., immersing the entire product in a water tank, using a water jet, and so on) still have cost and schedule issues.

Laser ultrasonic testing (LUT) is breakthrough technique. A laser pulsed light generates ultrasonic waves on a material surface by thermal expansion at low incident power density (thermoelastic effect) or by vaporizing surface material at high incident power density (ablation) [1, 2]. In addition, another laser light coupled to an interferometer acquires ultrasonic waves as mechanical displacement of the material surface. Since LUT realizes instantaneous and contactless inspection without contacting any transducers with materials, it has many advantages in high efficiency and extensive application [2].

While a number of studies and applications of LUT for metal materials have been presented, the LUT for polymeric materials such as FRPs is still in the research phase. One of the main reasons is the low signal-to-noise ratio (SNR) of LUT compared with the conventional UT. In addition, polymeric materials are large attenuation material.

Dubois and Drake revealed that a laser light with a wavelength in the vicinity of 3.2 μm is optimal for ultrasonic generation in CFRPs [3]. This is because the absorption bands of carbon-hydrogen stretching vibration and oxygen-hydrogen stretching vibration in epoxy matrix exist in those wavelength range, and because the penetration depth of 50 ~100 μm in CFRPs yields efficient ultrasound generation. However, a laser with such a wavelength is not available in the market. Therefore, commercial lasers, e.g., an Nd:YAG laser [4-7] or a CO_2 laser [3] are used for LUT of CFRPs and some of them use transducers for detecting ultrasonic waves so as to improve SNR [4, 7].

Thus, we have developed the most efficient wavelength conversion device for generating 3.2 μm wavelength mid-IR pulsed light by pumping an optical parametric oscillator (OPO) using a Nd:YAG solid-state laser [8]. Since the wavelength conversion device and the solid-state laser are compact and robust, our mid-IR pulsed laser is the most suitable laser ultrasonic generation source for polymeric materials. Then, we have developed the LUT system composed of the Nd:YAG laser, the wavelength conversion device, and the laser interferometer for detecting ultrasonic waves. It was confirmed that the system can generated and received ultrasonic waves in CFRPs out of touch, and successfully detected un-bonded area by transmission C-scan mode [8].

The purpose of the present study is to evaluate the performance of the mid-IR LUT system in reflection mode. We investigated the effects of the CFRP and the laser properties on the generated ultrasonic waves. In addition, C-scan images by the system were also presented.

2 GENERAL SPECIFICATIONS

2.1 MID-INFRARED LASER ULTRASONIC TESTING SYSTEM

As shown in Fig. 1, the mid-infrared LUT system was composed of the Nd:YAG solid-state laser (Centurion Plus, Quantel), the OPO wavelength conversion device, the sample scanning XY stage, a laser ultrasonic observation system (AIR-1550-TWM, OPTECH VENTURES LLC.) . The laser delivers 1.064 μm wavelength pulsed light with the maximum energy of 50 mJ, the pulse width of 12 ns, the beam divergence of 8 mrad, and the maximum repetition rate of 100 Hz. The pulse light was input into the wavelength conversion device from the right side.

The technique of the wavelength conversion device using optical parametric oscillation (OPO) was previously described in detail [8]. A specially developed crystal, a periodic polled stoichiometric lithium tantalate crystal (PPSLT) was placed between two plano–plano resonator mirrors in the device. The Nd:YAG laser pulse as a pump light was input into the resonator and then two different wavelength pulsed light, idler and signal waves, were output from the opposite side of the resonator. The respective wavelengths of the idler and signal waves are decided by the wavelength of the pump laser, the grating pitch of the crystal, and the refractive indices of pump, idler, and signal wave depending on the temperature [8, 9]. In order to adjust the wavelength of the idler wave to 3.2 μm, the pitch was designed as 30.9 μm and the temperature was kept to 40ºC. The lengths and apertures of the crystal were 35 mm and 4 mm × 4 mm, respectively. The output idler wave was separated from the pump and the signal waves by filters.

In our system, the mid-IR pulsed laser or the Nd:YAG pulsed laser were selected for the ultrasonic generation source. The pulsed laser was directed to the surface of a sample on the XY stage. The energy density (fluence) of the pulsed laser is determined by the power, the repetition rate, and the beam area of laser. While the repetition rate was fixed to 100 Hz, the output of the Nd:YAG solid-state laser were controlled to adjust the fluence of the mid-IR laser was almost the same as that of the Nd:YAG laser. The power and beam area on the stage were precisely measured by a power meter and beam profilers (Pyrocam III for mid-IR laser and SP620U for Nd:YAG laser, Ophir Optronics Solutions Ltd.), respectively. Note that while the beam shape of the Nd:YAG laser was a 2.5-mm square, that of the mid-IR laser was Gaussian with 1.9-mm diameter.

The ultrasonic waves at the same as the ultrasonic generation laser spot were detected by the laser

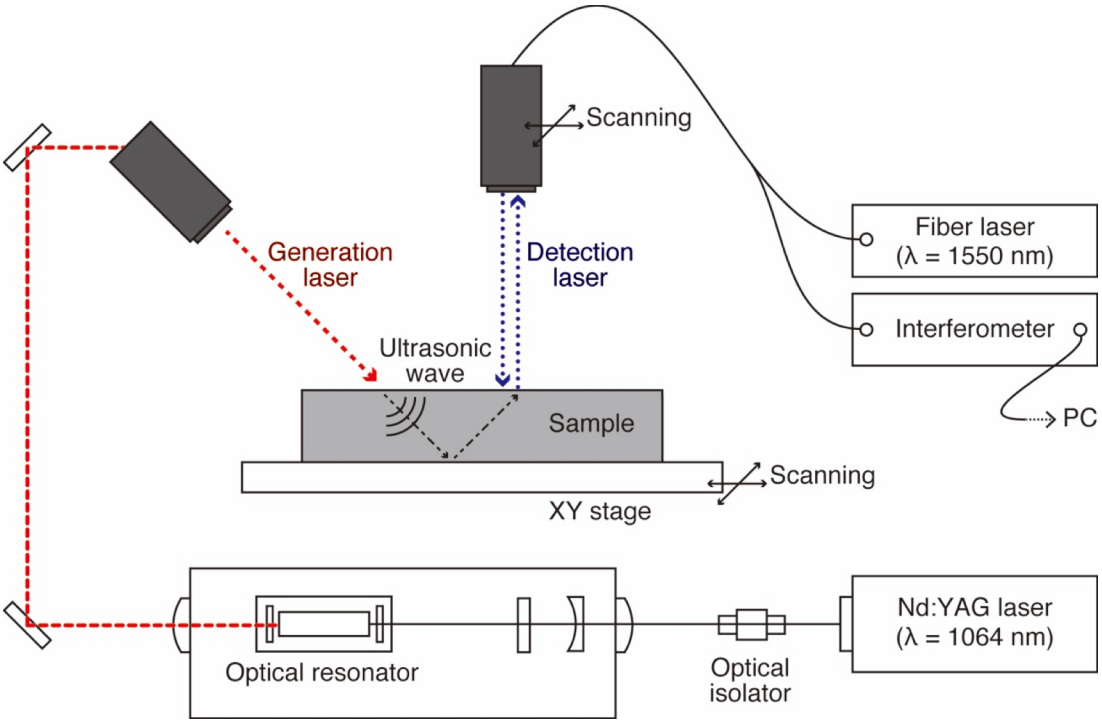

Fig. 1 The schematic image of the mid-IR laser ultrasonic system.

ultrasonic detection system (AIR-1550-TWM). The system is based on an adaptive interferometer using two-wave mixing in a photorefractive crystal [10]. A source laser (wavelength 1.55 μm) generates a reference beam and a signal beam. The signal beam directed onto sample reflects there and then is delivered to the photorefractive crystal. The reference beam is also directed onto the crystal at an angle to the signal beam. The two beams interfere in the crystal to produce a real-time hologram. When the surface of the work piece is displaced as a result of an ultrasonic excitation, the signal beam induces a transient phase change which is linearly converted into an amplitude change. At low frequencies, the amplitude decreases with frequency and reaches to 50% of the maximum at 100Hz – 1kHz. At high frequencies, the amplitude is independent of frequency and the photodetector determines the upper limit of the frequency as 125 MHz. The displacement signal by the laser ultrasonic detection system processed and converted to an ultrasonic velocity signal. Then, the velocity signal was analyzed using a 500 MHz oscilloscope (Wave Runner 6050A, LeCroy Corporation). The signal was averaged 100 times to reduce random noise. Moving XY stage or scanning head realized C-scan measurement.

2.2. SAMPLES

Two types of CFRP laminates, 1-mm isotropic and 3-mm plain-woven (Fig. 2(a) and (b), respectively), were measured by the LUT system. One side surface of the isotropic laminate was coated by an epoxy resin to evaluate the effects of the material surface (see the right sample in Fig. 2 (a)). A

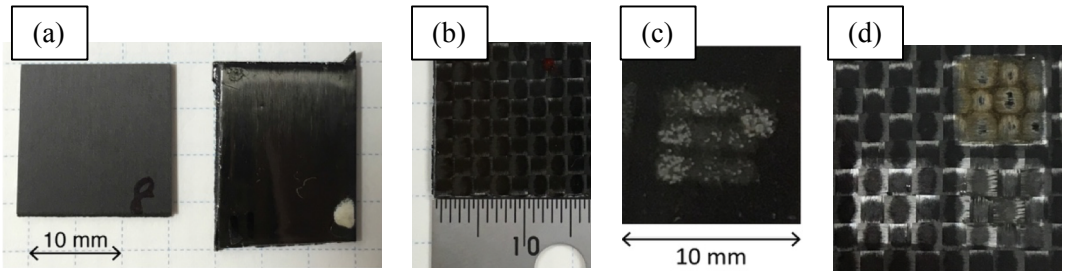

Fig. 2 (a) The isotropic CFRP laminate without and with epoxy coating and (b) the plain-woven CFRP laminate. The damaged surface by the YAG laser: (c) the isotropic and (d) the plain woven.

spin coater was used to coat the uniform thick epoxy resin (~ 30 μm) on the laminate. In addition, the LUT system tried to detect a PTFE sheet (5 mm × 5 mm) in the middle layer of a 2-mm isotropic CFRP laminate. The PTFE sheet was regarded as delamination in the laminate.

2.3 THRESHOLD OF DAMAGE TO CFRP IN TRANSMISSION MODE

When a laser illuminate a sample, the laser energy absorbed by the sample turns into heat energy and raise the temperature. Since the temperature rise generates the displacement variation on the sample surface, high laser energy can generate large ultrasonic waves. However, too much laser energy causes damage on the sample surface as demonstrated in Fig. 2 (c) and (d). Even though such surface damage cannot result in fatal effects on mechanical properties, the fluence should be less than damage threshold. While more than 0.06 J/cm^2 of the Nd:YAG laser left damage on the isotropic CFRP laminate, the mid-IR laser did not cause any damage or mark on the surface when the fluence was around 0.18 J/cm^2. Thus, the effect of laser fluence on ultrasonic waves in reflection mode and surface damage was measured.

The high damage threshold can be attributed to the low penetration depth of the YAG laser light into epoxy matrix. While more than 80% of the YAG laser energy penetrated through a 2-mm thick epoxy resin, the half of the mid-IR energy was absorbed by a 50-um thick epoxy. When a Nd:YAG laser light illuminates a CFRP sample, the laser energy is mainly absorbed by carbon fibers, which leads to local temperature increase likewise laser cutting. Thus, the YAG laser light is subject to damage. By contrast, the mid-IR laser light is absorbed by the epoxy matrix of the CFRP laminate and generates gentle temperature distribution in the laminate. Since the damage threshold of the mid-IR laser light should be three times as large energy as that of the YAG laser light at least, the mid-IR LUT system can generate larger ultrasonic waves and improve the SNR.

3. RESULTS

3.1 ULTRASONIC WAVES OF CFRP IN REFLECTION MODE

First, the isotropic CFRP laminate without epoxy coating was measured by the LUT system. As shown in Fig. 3, a peak, which is considered to be a longitudinal wave, was observed around 0.9 μs. However, the amplitude was too low to identify the shape of the signal masked by noises. Then, the isotropic CFRP laminate with the 30-μm thick epoxy coating was also measured in the same way. The waveforms in Fig. 4 shows the amplitude of the signal dramatically increased. In addition, pulsed signals around 1.5 – 1.7 μs and 2.3 – 2.5 μs were multiple reflection waves in the laminate. Note that the signals between 0.1– 0.3 μs were due to the reflection of the generation laser. The sound velocity of the laminate based on the time difference between these pulse signals (0.7 – 0.8 μs) was calculated as approx. 2700 m/s and corresponded with the common longitudinal ultrasonic velocity of CFRPs.

Fig. 5 shows the amplitude (the difference between the maximum and minimum amplitudes) of the 1st pulsed signal around 0.9 μs increased with the epoxy coating thickness and the fluecne of the laser, respectively. These results indicate that surface epoxy matrix of CFRPs significantly influences the SNR

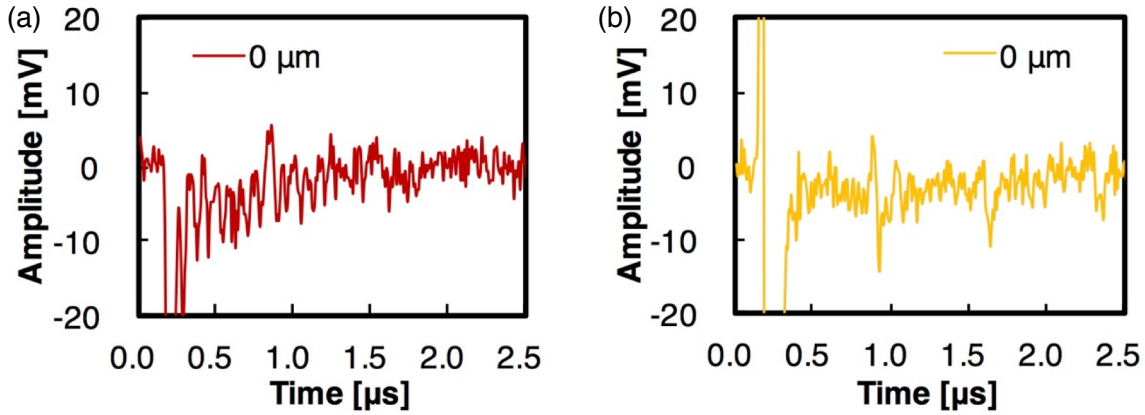

Fig. 3 The ultrasonic waveforms of the isotropic CFRP laminate without epoxy coating generated by (a) the mid-IR laser and (b) the Nd:YAG laser.

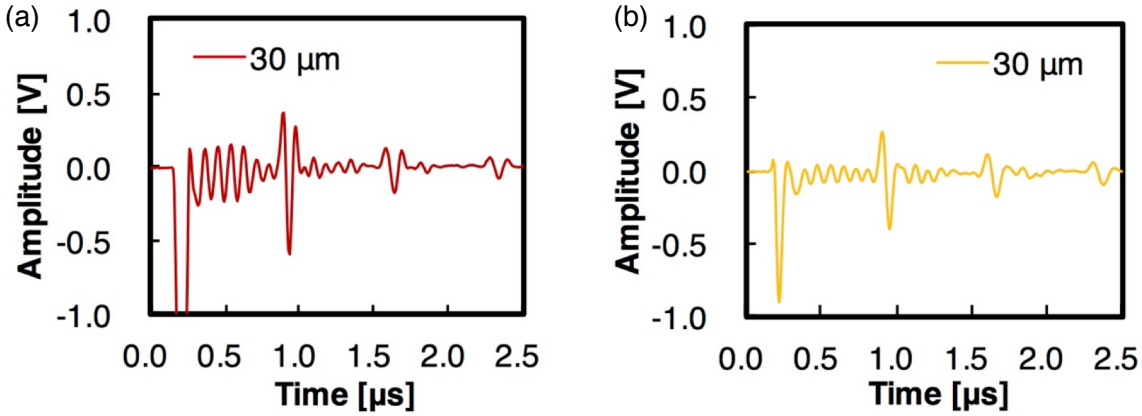

Fig. 4 The ultrasonic waveforms of the isotropic CFRP laminate with 30 μm epoxy coating generated by (a) the mid-IR laser and (b) the Nd:YAG laser.

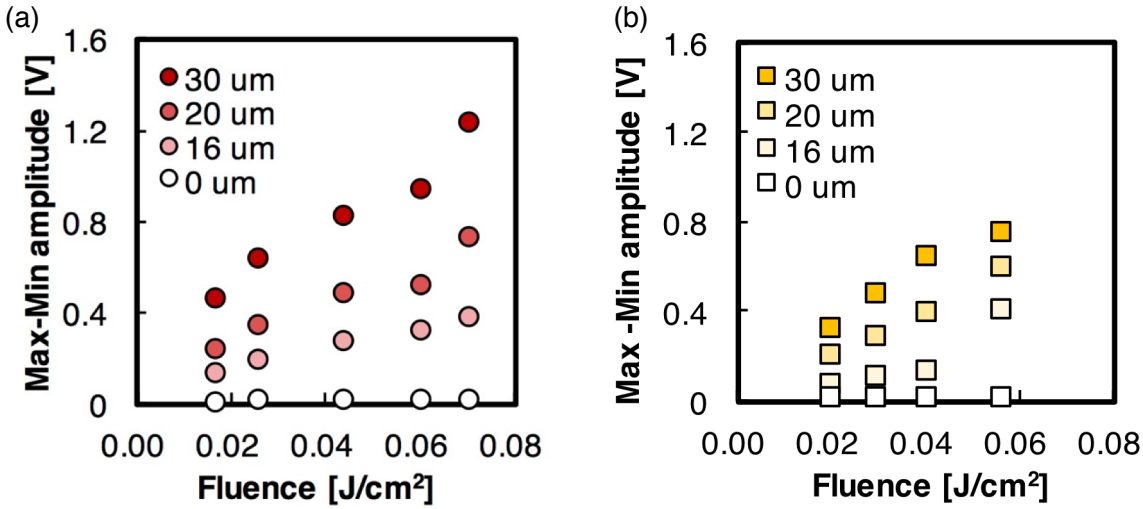

Fig. 5 The amplitude of the peak around 0.9 μs with the laser fluence: (a) the mid-IR laser and (b) the YAG laser.

of the LUT system. Although the damage threshold of the mid-IR laser should be above 0.18 J/cm^2 at least, the maximum fluence of the mid-IR laser was 0.07 J/cm^2 in the present reflection setup. Thus, the improvement of the system to increase the fluence will enhance the SNR.

3.2 C-SCAN IMAGE BY MID-IR LUT

Fig. 6 shows the waveforms and C-scan image of the 3-mm plain-woven CFRP laminate. The image was constructed based on the amplitude of the bottom echo, which appeared between 2.1 – 2.3 μs in Fig. 6 (a) and (b). As shown in Fig. 2 (b), the surface looked a pattern of the plain-woven carbon cloth. The pattern affect the epoxy amount near the surface: epoxy rich areas on the center of the carbon fiber bundle lattice, and carbon fiber rich areas on the bundle. As described in the previous section, the ultrasonic wave amplitude increases with the surface epoxy matrix so that the C-scan image was in accordance with the surface cloth pattern. While the ultrasonic echo was large on the epoxy rich area (Fig. 6 (a)), the echo was masked by noises on the carbon fiber rich area (Fig. 8 (b)). Consequently, the C-scan image demonstrated the pattern that corresponded with the surface carbon cloth.

The CFRP laminate including PTFE sheet was also inspected by the mid-IR LUT system. The PTFE sheet was regarded as delamination in the laminate. On the center of the delamination part, the ultrasonic wave in Fig. 7 (b) shows a clear pulse signal between 1.0 – 1.3 μs. This signal was an echo reflected at the delamination in the 1.0 mm depth of the laminate. In contrast, on the area without delamination, a pulse signal appeared between 1.9 – 2.2 μs in Fig. 7 (a), which was the bottom echo reflected at the opposite surface. The positive and negative peaks in the waveforms were represented as yellow and dark

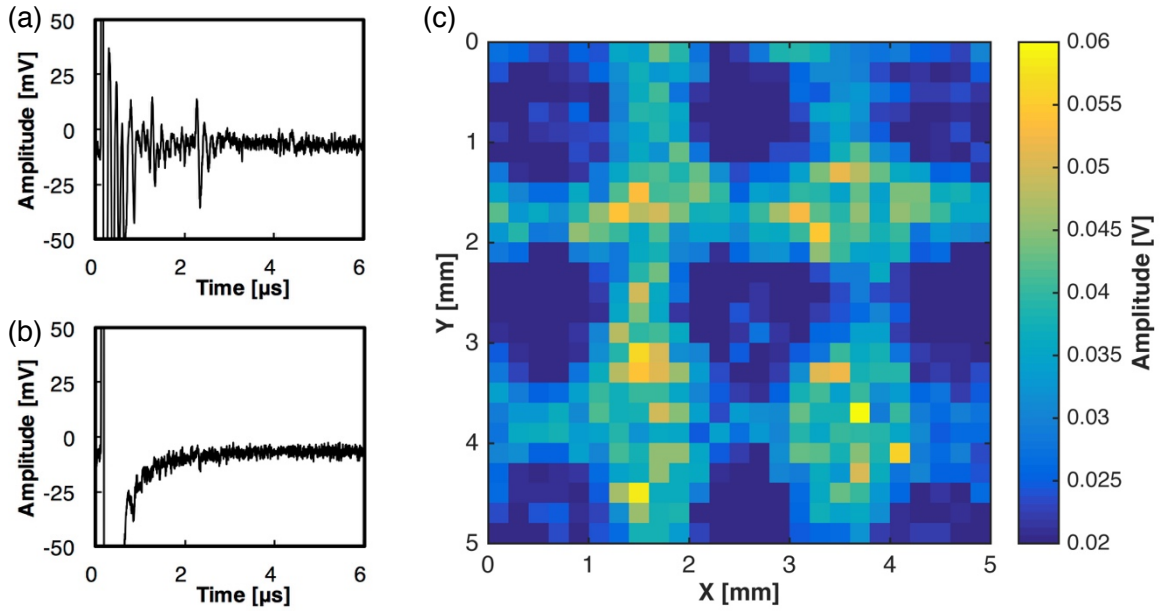

Fig. 6 The waveforms of the 3-mm plain woven CFRP laminate: (a) on the epoxy rich area and (b) on the carbon bundle. (c) The C-scan image constructed based on the amplitude between 2.1 2.3 μs.

blue in the B-scan image (Fig. 7 (c)). The image also shows the clear difference in the pulse echo time on the delamination (2 – 8 mm in the x axis) and the other area. As shown in Fig. 7 (d) and (e), two types of C-scan images were constructed by using 1.0 – 1.3 μs and 1.9 – 2.2 μs, respectively. Both the images showed a distinct contrast between the delamination (5 mm × 5 mm) and the other area. Besides, a peculiar pattern in the delamination area appeared in Fig. 7 (d). This may be attributed to waving of the PTFE sheet in the CFRP laminate.

3.3. DISCUSSION

In this work, we used the reflection mode of the mid-IR LUT system because it is more practical for NDT. It was found that our system can inspect 3-mm thick CFRP laminates and detect delamination in the laminate. However, the mid-IR LUT system has still potential to generate larger ultrasonic waves because three times the present maximum laser fluence should not damage the laminates. Thus, we can develop the system further to inspect a thicker sample and improve the SNR. One of the minor methods is reducing the loss of the energy by re-designing the optical path, but the effect is limited.

A fundamental idea to improve the system is to increase the wave conversion efficiency for raising the mid-IR laser energy. In fact, we have developed the most efficient wave conversion device which uses a two crystal OPO + difference frequency mixing (DFM) nonlinear wavelength conversion scheme [11]. Installing the device to the LUT system can realize thicker laminates inspection and highly-developed wave analyses.

4. CONCLUSIONS

The mid-IR LUT system can inspect the 3-mm thick CFRP laminate and detect delamination. The laser generated waves depends on the epoxy matrix near the laminate surface and the laser energy. Future research will focus on improving the SNR of the system and developing the wave analyses for the practical application.

ACKNOWLEDGEMENT

This research was supported by the Structural Materials for Innovation of the Cross Ministerial

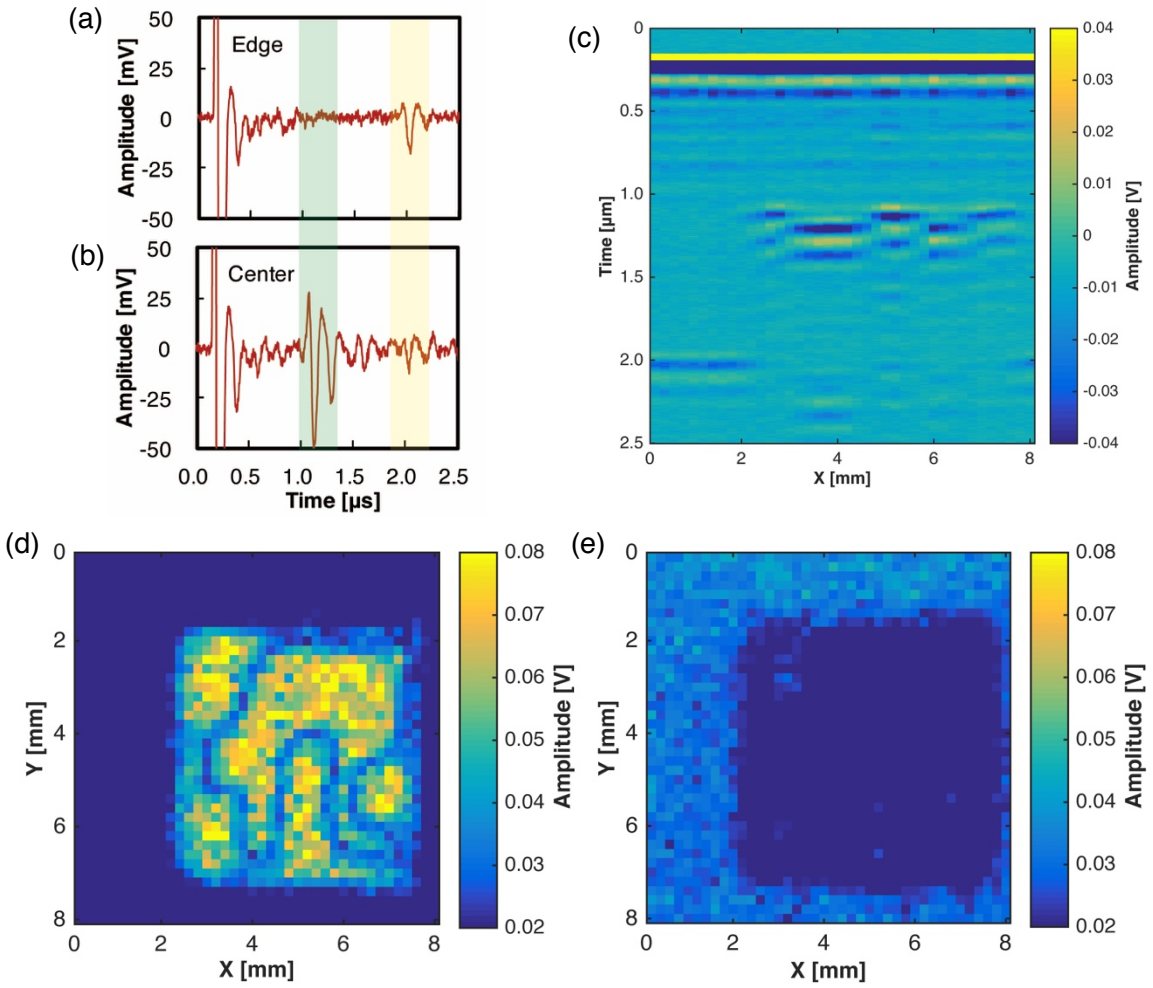

Fig. 7 The waveforms of the isotropic CFRP laminate including the PTFE sheet: (a) on the edge of the laminate and (b) on the delamination area (center). (c) The B-scan image. The C-scan image constructed based on the amplitude (d) between 1.0 1.3 μs and (e) between 1.9 – 2.2 μs.

Strategic Innovation Promotion Program (SIP) of Japan Science and Technology (JST). The authors acknowledge Dr. Nobuyuki Toyama (AIST) for CFRP laminates in this work.

REFERENCES

[1] J.D. Aussel, A.L. Brun, and J.C. Baboux, Generating acoustic waves by laser: theoretical and experimental study of the emission source, *Ultrasonics*, **26**, 1988, pp. 245–255 (DOI: 10.1016/0041-624X(88)90013-3).
[2] S.J. Davies, C. Edwards, G.S. Taylor, and S.B. Palmer, Laser-Generated Ultrasound - Its Properties, Mechanisms and Multifarious Applications, *Journal of Physics D: Applied Physics*, **26**, 1993, pp. 329–348.
[3] M. Dubois and T.E. Drake, Evolution of industrial laser-ultrasonic systems for the inspection of composites, *Nondestructive Testing and Evaluation*, **26**, 2011, pp. 213–228 (DOI: 10.1080/10589759.2011.573552).
[4] F.L. Di Scalea and R.E. Green, A hybrid non-contact ultrasonic system for sensing bond quality in tow-placed thermoplasitc composites, *Journal Composite Materials*, **34**, 2000, pp. 1860–1880 (DOI: 10.1106/LM8N-P39H-Y4QR-EWVP).
[5] C.C. Chia, J.R. Lee, C.Y. Park, and H.M. Jeong, Laser ultrasonic anomalous wave propagation imaging method with adjacent wave subtraction: Algorithm, *Optics & Laser Technology*, **44**, 2012, pp. 1507–1515 (DOI: 10.1016/j.optlastec.2011.12.008).

[6] B. Park, Y.K. An, and H. Sohn, Visualization of hidden delamination and debonding in composites through noncontact laser ultrasonic scanning, *Composites Science and Technology*, **100**, 2014, pp. 10–18 (DOI: 10.1016/j.compscitech.2014.05.029).
[7] H.J. Shin and J.R. Lee, Development of a long-range multi-area scanning ultrasonic propagation imaging system built into a hangar and its application on an actual aircraft, *Structural Health Monitoring*, **16**, 2016, pp. 1–15 (DOI: 10.1177/1475921716664493).
[8] H. Hatano, M. Watanabe, K. Kitamura, M. Naito, H. Yamawaki, and R. Slater, Mid IR pulsed light source for laser ultrasonic testing of carbon-fiber-reinforced plastic, *Journal of Optics*, **17**, 2015, pp. 1–8 (DOI: 10.1088/2040-8978/17/9/094011).
[9] H.H. Lim, S. Kurimura, T. Katagai, and I. Shoji. Temperature-Dependent Sellmeier Equation for Refractive Index of 1.0 mol % Mg-Doped Stoichiometric Lithium Tantalate, *Japanese Journal of Applied Physics*, **52**, 2013, 032601-1–4 (DOI: 10.7567/JJAP.52.032601).
[10] M.B. Klein, G.D. Bacher, A. Grunnet-Jepsen, D. Wright, and W.E. Moerner, Homodyne detection of ultrasonic surface displacements using two-wave mixing in photorefractive polymers. *Optics Communications*, **162**, 1999, pp. 79–84 (DOI: s10.1016/S0030-4018(99)00023-1).
[11] H. Hatano, R. Slater, S. Takekawa, M. Kusano, and M. Watanabe, Optimization of Mid-IR Generation from a PP-MgSLT Optical Parametric Oscillator with Intracavity Difference Frequency Mixing, *Japanese Journal of Applied Physics* (accepted).